

EXPERIMENTAL STUDY OF FATIGUE CRACK GROWTH  
UNDER BIAXIAL LOADING

M. Truchon\*, M. Amestoy\*\*, K. Dang-Van\*\*

\* Institut de Recherches de la Sidérurgie Française (IRSID)  
185, Rue du Président Roosevelt 78105 Saint Germain en Laye (France)  
\*\* Ecole Polytechnique, Laboratoire de Mécanique des Solides  
91120 Palaiseau (France)

ABSTRACT

This paper describes a test rig which allows development of a uniform biaxial stress field in the central part of a cruciform specimen. Experimental work was carried out on a C-Mn steel ( $\sigma_y = 360 \text{ N/mm}^2$ ) to study the influence of biaxiality on the growth of mode I fatigue cracks and the influence of bimodality on their directional stabilities.

KEYWORDS

Biaxial loading ; fatigue crack growth ; mixed-mode crack.

INTRODUCTION

The use of linear elastic fracture mechanics (LEFM) in the analysis of fatigue crack growth is well established on the basis of experiments carried out under uniaxial loads in such a way that cracks propagate in mode I. It has been shown that such cracks will propagate without deviation, and that the fatigue crack growth rate (FCGR) is a power function of the amplitude of stress intensity factor :

$$\frac{da}{dN} = C(\Delta K_I)^m$$

However, pressure vessels, pipe lines, aircraft skin structures, tubular nodes in an offshore platform, etc... are generally under a state of multiaxial stresses. If we consider a crack propagating in a biaxial stress field, several questions arise regarding :

1. the crack path. In the literature, it has been shown that mainly two factors can influence the crack path :
  - the existence of a mode II stress intensity factor, which has been discussed in the static case by many authors (Wu, 1978 ; Bilby and Cardew, 1975 ; Bilby, Cardew, Howard, 1977 ; Amestoy, Bul, Dang-Van, 1981 ; Erdogan, Sih and Bas, 1963 ; Hussain, Pu and Unterwood, 1974 ; Nuismer, 1975 ; Howard, 1978).
  - the existence of the non-singular stress if  $K_{II} = 0$ , which has been discussed by other authors (Cotterell, 1966 ; Leever, Radon, Culver, 1976 ; Kibler and Roberts, 1970 ; Streit and Finnie, 1979).
2. the fatigue crack growth rate (FCGR). Experimental studies have variously suggested that the stress parallel to the crack can increase (Joshi, Shewchuck, 1970), have no effect (Liu, Allison,

Dittmer, Yamane, 1979 ; Kitagawa, Yuuki, Tohgo, 1979) or decrease the FCGR (Leevers, Culver, Radon, 1979 ; Hopper, Miller, 1977).

EXPERIMENTAL CONDITIONS

Material

The experimental work was carried out on a E36-Z steel (AFNOR Standard) which is generally used in the construction of offshore platforms. This material was hot-rolled into plates of 20 mm thickness. Its chemical composition and mechanical properties are given in Tables 1 and 2.

TABLE 1. Chemical Composition of the E36-Z steel.

C	Mn	Si	S	P	Ni	Cr	Mo	Al	N2
0.145	1.40	0.292	0.003	0.006	0.42	0.075	0.031	0.019	0.012

TABLE 2. Mechanical Properties.

$\sigma_y$ (N/mm <sup>2</sup> )	$\sigma_{UTS}$ (N/mm <sup>2</sup> )	Elongation to rupture (%)	Reduction in Area (%)
370	530	33.5	75

Description of the Test Rig

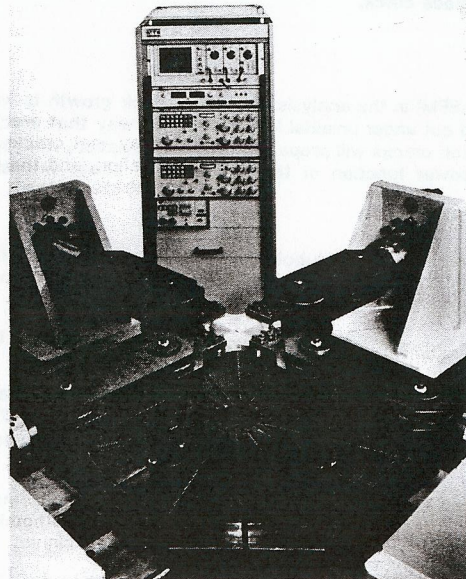


Fig. 1. Biaxial test rig.

The machine used for the experiments is described in Fig. 1. It is a horizontal machine with two actuators (250 kN dynamic capacity for each) pulling in two perpendicular directions. At the present time, it is possible to apply in-phase loads in the two directions or to vary one load, while maintaining the other constant. In any cases static and dynamic loads can be adjusted separately in the two directions.

With this testing equipment, the specimen must leave the center of the machine when loads are applied. In order to avoid bending of the specimen, two roller-bearings are supplied on each loading arm.

Specimen

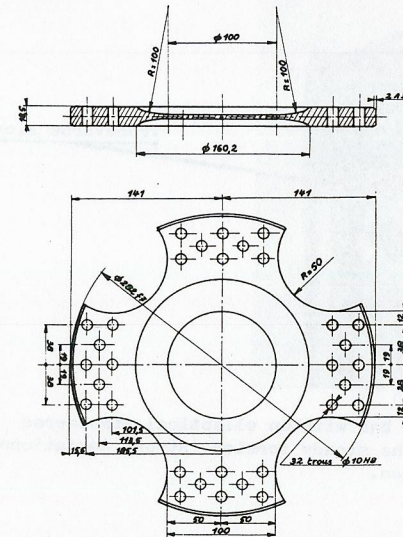


Fig. 2. Biaxial test specimen.

The specimen (Fig. 2) used was of cruciform shape. It was 20 mm thick throughout except for the central part which was 4.2 mm thick, over a diameter of 100 mm. At the center of the specimen, a notch 15 mm long, was machined. It could be oriented in any direction with respect to the loading arms.

Specimen Calibration

Strain gages and finite element method (F.E.M.) calculations (Gerald, Nguyen, 1978) were used to derive the principal stresses at the center of the cruciform specimen without a crack, and to determine the extent of the zone where the stress field is uniform.

The result of this calibration is shown in Fig. 3. It gives the variations of  $\frac{\sigma_1}{F_1}$  and  $\frac{\sigma_2}{F_1}$  as a function of the load biaxiality  $\frac{F_2}{F_1}$ . A regression analysis applied to strain gages measurements gives :

$$\begin{cases} \frac{\sigma_1}{F_1} = 1.409 - 0.423 \frac{F_2}{F_1} \\ \frac{\sigma_2}{F_1} = -0.453 + 1.496 \frac{F_2}{F_1} \end{cases} \quad (F \text{ in kN and } \sigma \text{ in N/mm}^2)$$

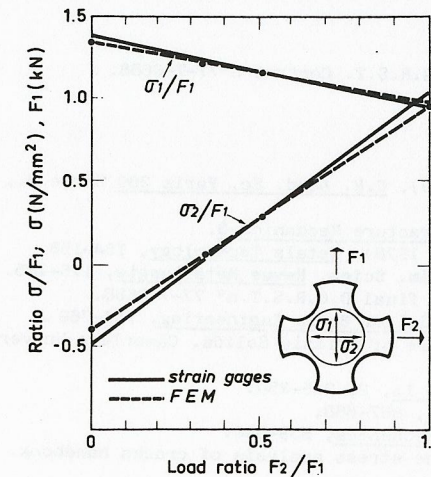


Fig. 3. Calibration of the cruciform specimen used for biaxial studies.

Figure 3 shows also that strain gages measurements agree with F.E.M. calculations. At last, it is important to notice that :

- the stress biaxiality varies from -0.35 to 1 when the load biaxiality varies from 0 to 1 ;
- the principal stresses are parallel to the applied loads.

The stress field uniformity was analysed by Gerald and Nguyen (1978) only with the help of F.E.M. in the equibiaxial configuration. In this configuration,  $\sigma_1$  should be equal to  $\sigma_2$ .

As shown in Fig. 4, the difference of the principal stresses values is less than 5% within 60% of the useful zone of the specimen.

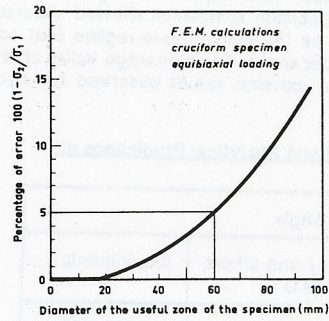


Fig. 4. F.E.M. analysis of the biaxial stress field uniformity in the equibiaxial case.

In order to take into account the finite specimen dimensions, a geometry factor  $F$  must be applied :

$$K_I = F \times \sigma_1 \sqrt{\pi a}$$

Uniaxial FCGR experiments were carried out on the cruciform specimen, the results of which were identified to those obtained with CT specimens on the same material for the same load ratio  $R = \frac{P_{min}}{P_{max}} = 0.1$ , following a procedure described on Fig. 5. It was found :  $F = 1.101 - 0.42 \frac{2a}{D}$  where  $D$  is the diameter of the specimen useful zone.

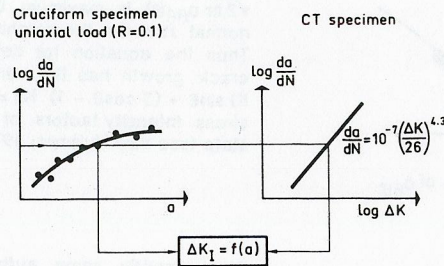


Fig. 5. Experimental determination of  $K_I$  for mode I fatigue cracks propagating in the cruciform specimen.

**Fatigue Crack Growth Monitoring**

In all cases, we used crack propagation gages to monitor the crack length by increments of 1 mm. When the crack was supposed to deviate from its initial direction, the gage was stuck in the direction predicted by an analytical criterion (see par. "Mechanical analysis").

**Specimen Calibration with a Fatigue Crack.**

For the inclined crack under biaxial load in an infinite sheet,  $K_I$  and  $K_{II}$  are given by the following formulae :

$$K_I = \frac{1}{2} \sigma_1 \sqrt{\pi a} \left[ 1 + \frac{\sigma_2}{\sigma_1} - \left( 1 - \frac{\sigma_2}{\sigma_1} \right) \cos 2\alpha \right]$$

$$K_{II} = \frac{1}{2} \sigma_1 \sqrt{\pi a} \left( 1 - \frac{\sigma_2}{\sigma_1} \right) \sin 2\alpha$$

where  $\alpha$  is the angle between  $\sigma_1$  and the crack.

In the particular case where the initial crack is perpendicular to the maximum principal stress  $\sigma_1$ ,  $K_{II}$  is reduced to zero and  $K_I = \sigma_1 \sqrt{\pi a}$  for any value of  $\frac{\sigma_2}{\sigma_1}$ .

**EFFECT OF BIAxIAL LOAD ON MODE I FCGR**

**Definitions and Test Conditions**

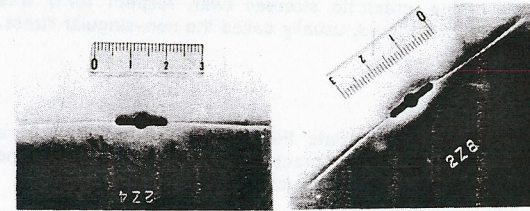
$-\sigma_x$  is the principal stress parallel to the crack.

$-\sigma_y$  is the principal stress perpendicular to the crack.

Biaxiality ratio  $B = \frac{\sigma_x}{\sigma_y}$ . In all the experiments of this work, this ratio is constant at any moment of the load cycle. This means that the loads were applied in phase, with the same load ratio  $R$  which induces the same stress ratio  $R = \frac{\sigma_{x_{min}}}{\sigma_{x_{max}}} = \frac{\sigma_{y_{min}}}{\sigma_{y_{max}}} = 0.1$ .

Mode I fatigue cracking can be obtained either with a crack parallel to a principal stress, whatever the biaxiality ratio, or in the equibiaxial case whatever the crack direction.

**Fatigue Crack Growth when  $\sigma_x < \sigma_y$**



The crack was found to grow straight when the maximum principal stress was normal to it, as shown on fig. 6.

Fig. 6. Some examples of fatigue cracks propagating under mode I conditions in a biaxial stress field where  $\sigma_x \leq \sigma_y$ .

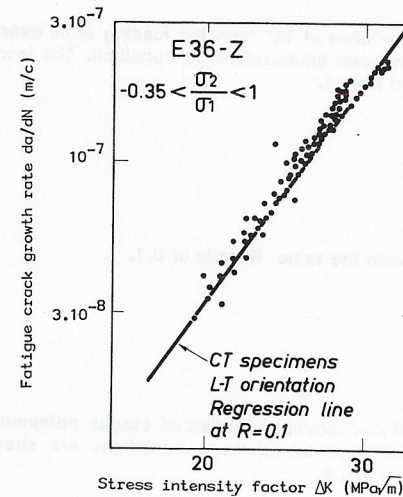


Figure 7 also shows the variations of FCGR as a function of  $\Delta K_I$  during these experiments. They were all carried out in the same range of  $\Delta K_I$  values, but for different values of the stress biaxiality  $B = \frac{\sigma_x}{\sigma_y}$  ranging from  $-0.35$  to  $1$ . It can be seen that the ratio  $B$  has no influence on the fatigue crack growth rates observed.

The conclusion that can be drawn from these results is that the FCGR under biaxial loading can be correctly described by the same Paris equation as in the uniaxial case provided there is no deviation of the crack ( $K_{II} = 0$ ) and that the stress parallel to the crack is lower than the normal stress.

Fig. 7. Comparison between FCGR obtained under uniaxial and biaxial loading conditions.

Fatigue Crack Growth when  $\sigma_x > \sigma_y$

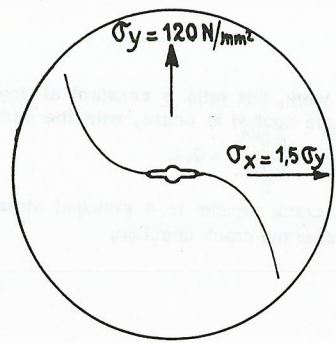


Fig. 8. S-shaped crack path in a biaxial stress field where  $\sigma_x > \sigma_y$ .

However, because no exact analytical solution can calculate the stress intensity factor of a S-shaped crack, it is neither possible to predict the amount of crack curvature with respect to the non-singular stress, nor to analyse the FCGR results obtained in such conditions.

GROWTH OF MIXED-MODE FATIGUE CRACKS

Test Conditions

Tests were carried out on cruciform specimens with notches at 45° from the loading arms direction. They were precracked on 3 mm from the notch under equibiaxial load condition. The loads were then changed to have a stress biaxiality different from 1.

The stress intensity factors become :

$$K_I = \frac{1}{2} \sigma_1 \sqrt{\pi a} \left( 1 + \frac{\sigma_2}{\sigma_1} \right)$$

$$K_{II} = \frac{1}{2} \sigma_1 \sqrt{\pi a} \left( 1 - \frac{\sigma_2}{\sigma_1} \right)$$

Like previously, stresses were applied in-phase and with the same R ratio of 0.1.

Test Results

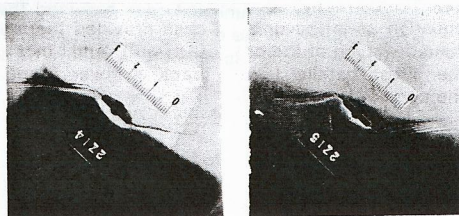


Fig. 9. Examples of kinked crack  
a.  $\sigma_2/\sigma_1 = 0.435$  b.  $\sigma_2/\sigma_1 = -0.32$ .

Figure 8 shows a typical result of FCG when the biaxiality ratio B is more than unity. In this case, it was equal to  $B = 1.5$  with a stress ratio R in the two directions equal to 0.1. As many authors (Leevers, Radon, Culver, 1976 ; Liu and co-workers, 1979 ; Kitagawa and co-workers, 1979), we observed that the crack propagated along an S-shaped path. It must be emphasized that this crack path does not present any tangential discontinuity. For this reason, such a crack must not be considered as a mixed-mode crack.

Some authors (Cotterell, 1966 ; Streit and Finnie, 1979 ; Finnie and Saith, 1973) mentioned that such a phenomenon could be described if the finite term of the power series development of the crack tip stresses (with respect to  $\sqrt{r}$ ) was considered, usually called the non-singular stress.

From the experiment no 2Z-14, it can be noticed that the crack path after kinking may not remain straight, but tends toward the perpendicular direction to the maximum principal stress, that is to become a mode I fatigue crack. This is the reason why in the table 3, the measured angles refer to the first steps of the kinked crack, to be compared to the analytical predictions.

The experimental crack paths were observed with an optical microscope at a magnification of 50. Kink angles measured on the two faces of the same specimen sometimes showed different values : specimen 2Z-9 for example. A reason for this may be the plane-stress regime that can develop at the crack tip, because of the reduced specimen thickness. As an average value of the kink angle has no physical meaning, Table 3 only gives the extreme values observed for each experiment.

TABLE 3. Comparison between Experimental Results and Analytical Predictions of the Kink Angle.

Specimen	$\frac{\sigma_2}{\sigma_1}$	Kink angle		
		Erdogan - Sih (1963)	Amestoy and others (1981)	Experimental
2Z-15	-0,32	61°	66°	57°-65°
2Z-9	0,06	51,5°	55°	57°-59°
2Z-14	0,435	35,5°	36°	35°-36°
2Z-11	0,54	29°	30°	20°-23°

Mechanical Analysis

Let us consider an elastic body in plane-state condition : many authors have attempted to predict branching which appears in experiments of mixed-mode fatigue crack propagation.

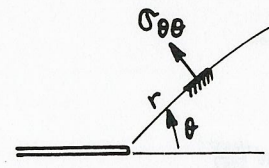


Fig. 10. Definition of  $\sigma_{\theta\theta}$

A first criterion (approximate) was proposed by Erdogan and Sih (1963) who assume that the crack will develop in the direction  $\theta = \theta_0$  for which  $\sqrt{2\pi r} \sigma_{\theta\theta}(\theta)$  is maximum (Fig. 10) where  $\sigma_{\theta\theta}$  is the normal stress in the neighbourhood of the crack tip. Thus the equation for determining the direction of crack growth has the very simple analytical form :  $K_I \sin\theta + (3 \cos\theta - 1) K_{II} = 0$ , where  $(K_I, K_{II})$  are the stress intensity factors of the crack in the initial state (see also Nuismer, 1975 ; Howard, 1978).

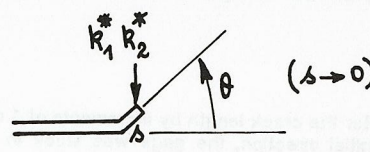


Fig. 11. Definition of  $k_1^*$  and  $k_2^*$

More recently some authors (Bilby and Cardew, 1975 ; Bilby and co-workers, 1977 ; Wu, 1978 ; Amestoy and others, 1981) have performed careful analysis of the kinked crack problem so that the criterion can be expressed by means of the exact analytical computation of the stress-intensity factors  $(k_1^*, k_2^*)$  which appear at the tip of an infinitesimal kink deviated of an arbitrary angle from the crack (Fig. 11).

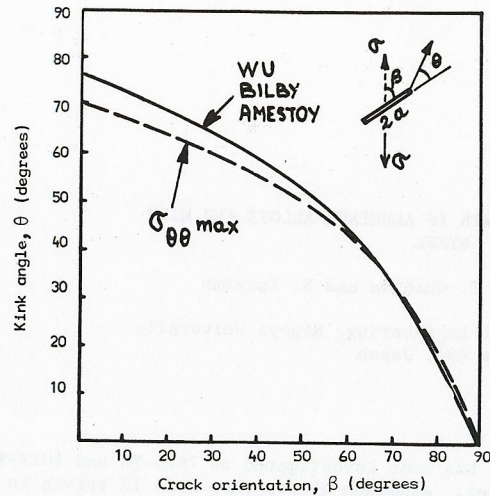


Fig. 12. Comparison of criteria commonly used to predict crack branching.

#### CONCLUSION

This paper describes the testing equipment which was used to study fatigue crack growth in a biaxial stress field.

Tests were carried out on a cruciform specimen which exhibited a useful zone of 60 mm diameter where the stress field was found satisfactorily uniform. Principal stresses were calculated with the help of strain gages or F.E.M.

From the experimental work carried out on an E36-Z steel (AFNOR Standard), the following conclusions can be drawn :

- The propagation path and FCGR of mode I fatigue cracks are not modified by the stress parallel to the crack  $\sigma_x$ , for biaxiality ratios  $\frac{\sigma_x}{\sigma_y}$  lower than unity.
- When  $\frac{\sigma_x}{\sigma_y}$  is greater than one, the crack is observed to take an S-shaped path.
- When  $K_{II} \neq 0$ , the crack is observed to kink with an angle which can be correctly predicted by analytical solutions.

#### REFERENCES

- Wu, C.H. (1978). *Journal of Applied Mechanics*, vol. 45, p. 553-558.
- Bilby, B.A. and G.E. Cardew (1975). *Int. J. of Fract.*, 11, p. 708-712.
- Bilby, B.A., G.E. Cardew and I.C. Howard (1977). *Fracture 77*, vol. 3. University of Waterloo Press, Canada, p. 197-200.
- Amestoy, M. H.D. Bui and K. Dang-Van (1981). *Proc. Int. Conf. Fract.*, Cannes, paper n° 348.

Erdogan, F., G.C. Sih (1963). *J. Bas. Engng.*, vol. 85, n° 4, p. 519-527.

Hussain, M.A., S.L. Pu and J.H. Underwood (1974). *ASTM STP 560*, p. 2-28.

Nuismer, R.J. (1975). *Int. J. of Fract.*, vol. 11, n° 2, p. 245-250.

Howard, I.C. (1978). *Int. J. of Fract.*, 14, p. R307-R310.

Cottrell, B. (1966). *Int. J. of Fract. Mech.*, vol. 2, n° 3, p. 526-533.

Leevers, P.S., J.C. Radon and L.E. Culver (1976). *J. Mech. Phys. Solids*, vol. 24, p. 381-395.

Kibler, J.J. and R. Roberts (1970). *Trans. ASME, J. Eng. Ind.*, p. 727-734.

Streit, R.D. and I. Finnie (1979). *Proc. of ICM 3*, Cambridge, vol. 3, p. 469-478.

Joshi, S.R. and J. Shewchuck (1970). *Exp. Mech.*, vol. 10, n° 12, p. 529.

Liu, A.F., J.E. Allison, D.F. Dittmer and J.R. Yamane (1979). *ASTM STP 677*, p. 5-22.

Kitagawa, H., R. Yuuki and K. Tohgo (1979). *Fatigue Engng. Mat. St.*, vol. 2, p. 195-206.

Leevers, P.S., L.E. Culver and J.C. Radon (1979). *Eng. Fract. Mech.*, vol. 11, p. 487-498.

Hopper, C.D. and K.J. Miller (1977). *J. Strain Analysis*, vol. 12, n° 1, p. 23-28.

Gerald, J. and Q.S. Nguyen (1978). Ecole Polytechnique, Laboratoire de Mécanique des Solides, rapport ANMT n° 6.

Finnie, I. and A. Saith (1973). *Int. J. Fract.*, 9, p. 484-486.